LA-UR- 96-2288

CONF-960713--2

Title: BUOYANCY-GENERATED VARIABLE-DENSITY TURBULENCE

Author(s): Donald L. Sandoval
Timothy T. Clark
James J. Riley

Submitted to: IUTAM Symposium on Variable Density Low-Speed Turbulent Flows
8 - 10 July 1996
Institut de Recherche sur les Phenomenes Hors Equilibre
Marseille, France

DISTRIBUTION OF THIS DOCUMENT IS UNLIMITED

Los Alamos
NATIONAL LABORATORY

Form No. 836 R5
ST 2629 10/91

DISCLAIMER

BUOYANCY-GENERATED VARIABLE-DENSITY TURBULENCE

D. L. SANDOVAL AND T. T. CLARK
Los Alamos National Laboratory
Los Alamos, New Mexico USA 87545

AND

J. J. RILEY
University of Washington
Seattle, Washington USA 98145

1. Introduction

Because of the importance of turbulence mixing in many applications, a number of turbulence mixing models have been proposed for variable-density flows, [see, e.g., Zeman and Lumley (1972), Andronov et al.(1982), Besnard et al. (1992), and Cranfill (1992)]. These engineering models (one-point statistical models) typically include the transport of the turbulent kinetic energy and the turbulent energy dissipation rate (i.e., $k-\epsilon$ models). The model presented by Besnard, Harlow, Rauenzahn and Zemach (1992) (herein referred to as BHRZ) is a one-point model intended to describe variable-density turbulent flows. Transport equations for the Reynolds stress tensor, R_{ij}, and the turbulent energy dissipation rate, the density-velocity correlation, a_i, and the density-specific volume correlation, b are derived. This model employs techniques and concepts from incompressible, constant-density turbulence modeling and incorporates ideas from two-phase flow models.

Clark and Spitz (1994) present a two-point model for variable-density turbulence. Their derivation is based on transport equations that are based on two-point generalizations of R_{ij}, a_i, and b. These equations are Fourier transformed with respect to the separation distance between the two points. Transport equations are derived for R_{ij}, a_i, b. As in the one-point model, this model contains many *ad-hoc* assumptions and unknown model coefficients that must be determined by comparison with experimental and nu-

merical data. However, the two-point formalism requires fewer equillibrium assumptions then does a single-point model.

Our primary concern in this paper lies in the nonlinear processes of turbulence and the influence of large density variations (not within the Boussinesq limit) on these processes. To isolate the effects of variable-density on the turbulence we restrict our flow to be incompressible, statistically homogeneous buoyancy-generated turbulence. To our knowledge there have not been any simulations reported for this problem.

2. Equations of Motion

We shall consider the turbulent mixing of two miscible, incompressible fluids of different densities. By incompressible fluid we mean a fluid whose compressibility coefficient and thermal expansion coefficient are both zero. This decouples acoustic waves from the problem, implying an infinite sound speed and that density is no longer a thermodynamic variable and therefore not a function of the pressure or temperature. The Mach number is zero. The velocity field for the mixing of two miscible, incompressible fluids is not in general divergence free, i.e., $\nabla \cdot \vec{u} \neq 0$ [Joseph (1990)]. Thus the flow in this study is incompressible due to the low Mach number criterion but the divergence of the velocity field is not zero.

The conservation of mass is

$$\frac{\partial \rho}{\partial t} + \frac{\partial \rho u_j}{\partial x_j} = 0. \tag{1}$$

The Navier-Stokes equations are

$$\frac{\partial \rho u_i}{\partial t} + \frac{\partial \rho u_i u_j}{\partial x_j} = -\frac{\partial p}{\partial x_i} + \frac{\partial \tau_{ij}}{\partial x_j} + \rho g_i \tag{2}$$

with the viscous stress tensor for a Newtonian fluid defined by

$$\tau_{ij} = \mu \left\{ \frac{\partial u_i}{\partial x_j} + \frac{\partial u_j}{\partial x_i} - \frac{2}{3}\delta_{ij}\frac{\partial u_n}{\partial x_n} \right\}.$$

Here ρ, p and u_i are the density, pressure and velocity fields, respectively, dependent on the spatial coordinate x_i and on time t, g_i is an acceleration (e.g., gravity), and μ the fluid viscosity, assumed constant. Fick's law [see, e.g., Bird, Stewart and Lightfoot (1960)] for the diffusion of two species of different densities gives

$$\frac{\partial \rho}{\partial t} + u_j \frac{\partial \rho}{\partial x_j} = \rho \frac{\partial}{\partial x_n} \left\{ \frac{\mathcal{D}}{\rho} \frac{\partial \rho}{\partial x_n} \right\} \tag{3}$$

Comparison of Eq. (1) with (3) leads to the following result for incompressible mixing flows:

$$\frac{\partial u_n}{\partial x_n} = -\frac{\partial}{\partial x_n}\left\{\frac{\mathcal{D}}{\rho}\frac{\partial \rho}{\partial x_n}\right\}. \tag{4}$$

Thus, the incompressible velocity field is divergent.

These equations will be solved with periodic boundry conditions and "random" initial conditions for density and a nearly zero initial velocity.

3. Averaged Equations

We examine homogeneous turbulence subjected to an acceleration. Letting a tilde denote a mass-weighted average and an overbar denote a volume-weighted average, we have

$$u_i = \overline{U}_i + u_i' = \tilde{U}_i + u_i''.$$

Where, $\tilde{u}_i = \overline{\rho u_i}/\overline{\rho}$. Note that $u_i'' = a_i + u_i'$ where $a_i = \overline{u_i''}$. The frame of motion is chosen so that the mean volume-weighted velocity is zero; $\overline{U}_i = 0 = \tilde{U}_i + a_i$. The exact averaged equations for the subsequent correlations are:

$$\frac{\partial R_{ij}}{\partial t} = a_i\frac{\partial \overline{P}}{\partial x_j} + a_j\frac{\partial \overline{P}}{\partial x_i} - \overline{u_j'\frac{\partial p'}{\partial x_i}} - \overline{u_i'\frac{\partial p'}{\partial x_j}} + \overline{u_j'\frac{\partial \tau_{ni}'}{\partial x_n}} + \overline{u_i'\frac{\partial \tau_{nj}'}{\partial x_n}} \tag{5}$$

$$\frac{\partial a_i}{\partial t} + \overline{u_n'\frac{\partial u_i'}{\partial x_n}} = -b\frac{\partial \overline{P}}{\partial x_i} - \overline{v'\frac{\partial p'}{\partial x_i}} + \overline{v'\frac{\partial \tau_{ni}'}{\partial x_n}} \tag{6}$$

and

$$\frac{\partial b}{\partial t} = -2\overline{v'\frac{\partial u_n'}{\partial x_n}}. \tag{7}$$

Where a_i is the turbulent mass flux, defined above, $b = -\overline{\rho' v'}/\overline{\rho}$ is the density-specific volume correlation, and R_{ij} is the mass-weighted Reynolds stress tensor, $R_{ij} = \overline{\rho u_i'' u_j''}$. The mass-weighted mean velocity, $\tilde{U}_i = -a_i$ is given by

$$\frac{\partial \tilde{U}_i}{\partial t} = -\frac{1}{\overline{\rho}}\frac{\partial \overline{P}}{\partial x_i} + g_i = -\frac{\partial a_i}{\partial t} \tag{8}$$

Then from Eqs. (6) and (8) and exploiting homogeneity;

$$\underbrace{\frac{\partial \overline{P}}{\partial x_i}}_{A} = \left(\frac{\overline{\rho}}{1-\overline{\rho}b}\right)\left\{\underbrace{g_i}_{B} + \underbrace{\overline{v'\frac{\partial \tau_{ni}'}{\partial x_n}}}_{C} - \underbrace{\overline{v'\frac{\partial p'}{\partial x_i}}}_{D} + \underbrace{\overline{u_i'\frac{\partial u_n'}{\partial x_n}}}_{E}\right\}. \tag{9}$$

Substituting (9) into (6), and in the limit of small time we neglect the velocities;

$$\frac{\partial a_i}{\partial t} = \left(\frac{\overline{\rho} b}{1-\overline{\rho} b}\right) g_i - \left(\frac{1}{1-\overline{\rho} b}\right) \overline{v' \frac{\partial p'}{\partial x_i}}. \tag{10}$$

The second term on the right side is modeled (e.g., in BHRZ) as a simple "drag" (i.e., a destruction of a_i). If this modeling is accurate, then this term is proportional to a_i, and hence asymptotically tends to zero in the limit of small time. The variations in this correlation can be studied via direct numerical simulation of equations (1) through (3) with (9). The simulations are used to compute;

$$\overline{v' \frac{\partial p'}{\partial x_i}} = \overline{\rho} b g_i + (\overline{\rho} b + 1) \frac{\partial a_i}{\partial t} = -\overline{p' \frac{\partial v'}{\partial x_i}}. \tag{11}$$

which may be plotted versus a_i to determine the appropriateness of an interpretation of drag.

4. Numerical Simulations

A numerical algorithm solving Eqs. (1) through (3) and (9) was developed from the algorithm of McMurtry (1987). It is modified for the incompressible mixing of miscible fluids subjected to a constant acceleration. This algorithm is related to the projection method but takes into account the fact that the velocity field is divergent. A pseudo-spectral method is used so that the spatial derivatives are computed in wavenumber space whereas the nonlinear terms are computed in physical space via the use of fast Fourier transforms. The aliasing errors are ameliorated by truncation of the Fourier fields. The temporal discretization is Adams-Bashforth and the fields are time-advanced in wavenumber space. As in the work of Batchelor, Canuto and Chasnov (1992), the fluctuations are assumed to be periodic in all three spatial directions. However, the Boussinesq approximation has not been made. Simulations used a grid size of 128^3.

4.1. NONDIMENSIONALIZATION

The equations of motion are solved in nondimensional form following Batchelor, et al. (1992). A statistical measure of the initial density variations is used; θ_o is a measure of the dimensionless density variations defined as

$$\theta_o = \left(\overline{\rho' \rho' / \rho_o^2}\right)^{\frac{1}{2}}_{T=0} = \rho^* / \rho_o.$$

Where ρ^* is the rms value of the initial density fluctuations. The length scale, l_o, characterizes the wavelength at which the initial spectrum of ρ'

has its maximum. That is, $l_o = 2\pi/k_m$, where k_m is the wavenumber at which the density spectrum is a maximum. For the density fields studied here, $k_m = 3$ so that $l_o = 2\pi/3$.

Again, following Batchelor, et al. (1992);

$$T = t\left(\frac{g\theta_o}{l_o}\right)^{\frac{1}{2}}, \quad \mathbf{X} = \frac{\mathbf{x}}{l_o}, \quad \mathbf{U} = \frac{\mathbf{u}}{(l_o g\theta_o)^{\frac{1}{2}}}.$$

For the pressure, total density, and fluctuating density:

$$\tilde{P} = \frac{P}{\rho_o l_o g\theta_o}, \quad \Theta = \frac{\rho}{\rho_o}, \quad \Theta' = \frac{\rho'}{\rho^*}.$$

Two nondimensional variables arise in the equations of motion. These are

$$R_o = \frac{\left(l_o{}^3 g\theta_o\right)^{\frac{1}{2}}}{\nu}, \quad \sigma = \frac{\nu}{\mathcal{D}}$$

where R_o is a measure of the drive strength and σ is the Schmidt number.

4.2. INITIAL CONDITIONS

The density field is initialized using the method of Eswaran and Pope (1988). This method creates an initial density field that approximately conforms to a double-delta function probability density function (pdf), where the density values of the initial field corresponds closely to either the high density or low density value.

The initial velocity field is set to zero, then slightly modified to account for the divergent velocity [eq. (4)] condition. Because the initial velocity field is nearly zero, density-velocity correlations are initially nearly zero. An acceleration is applied in the z-direction and the developing flow is statistically axisymmetric about the z-axis.

Figure 1 shows the evolution of the initial probability density function of the 3-D density fields for the two cases presented in this study. This shows that for the initial conditions a high probability for the density to be either ρ_{max} or ρ_{min} and also the "U-shaped" lower probability region in between the two peaks representing the premixed interface. Table 1 lists the initial density statistics for the simulations. Case NCD is a nearly constant-density case performed to provide comparisons with the fully variable-density case, FVD. The quantities $B(t) = \overline{\rho'\rho'}/\overline{\rho}^2$ and $b(t) = -\overline{\rho'(1/\rho)'}$ are nondimensional measures of the density variations in the flow. In the limit as the density fluctuations tend to zero $B(t) \approx b(t)$.

Run	R_o	ν	σ	g	ρ_{max}	ρ_{min}	ρ_{max}/ρ_{min}	θ_o
NCD	256	7.800e-3	1.0	10.	1.05	0.95	1.105	0.0434
FVD	256	8.543e-3	1.0	1.0	1.60	0.40	4.000	0.5206

TABLE 1. List of initial statistics for buoyancy-driven cases

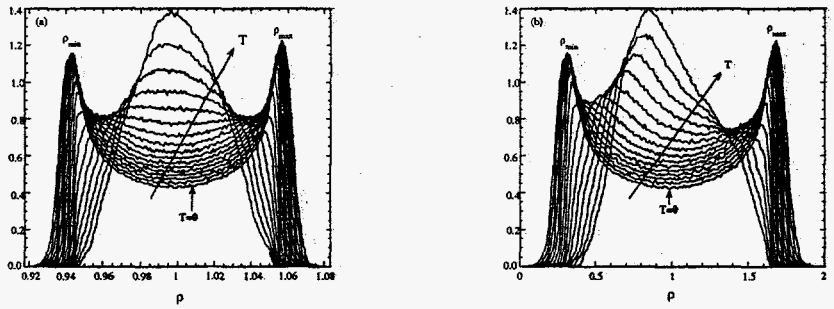

Figure 1. PDF evolution, for T=0.0 to 2.0 by 0.125, of the density field for (a) NCD case ($\theta_o = 0.04$) and (b) FVD case ($\theta_o = 0.52$) cases

5. Numerical Results

In the two cases considered, the initial conditions are such that R_o is the same in both cases but the initial density ratios are different. The initial velocity is nearly zero. Through the action of an acceleration, the velocity increases rapidly and the fluid is set into motion. The energy reaches a maximum and begins to decrease as the density field mixes and diffuses towards its constant mean value, and as viscous dissipation becomes appreciable. The velocity is initially highly correlated with the density field. The density field corresponds to a source of potential energy which is converted to kinetic energy ("turbulence") and finally into "heat" (viscous work). As the density field diffuses and mixes towards its mean value the source of potential energy decays and the remaining kinetic energy decays away. The kinetic energy will tend towards zero when the density field is uniformly mixed (there is no available potential energy) and dissipation removes the remaining kinetic energy.

Figure 1 shows the evolution of the pdf of the density field for the two cases presented. As time evolves and the flow develops, the density field is mixing through convective and molecular effects, and the bimodal pdf evolves towards a nearly Gaussian function whose maximum is at the mean

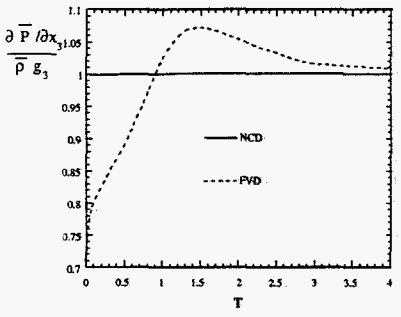

Figure 2. Evolution of the mean pressure gradient for both cases.

density of 1.0. For these cases the pdf is slightly skewed to the lower side of the mean density. The Boussinesq approximation for these flows predicts symmetric evolution of the PDF because both positive and negative density fluctuations receive the same acceleration. Comparing Fig. (1a) with (1b), the feature that immediately stands out is the skewed behavior of the pdf's as they evolve. For the case with $\theta_o = 0.52$, the pdf is more strongly skewed to the negative side of the mean density of 1 than it is for the $\theta_o = 0.04$ case. The physical explanation for this behavior possibly lies in the entrainment rates of the heavy and light fluid into the mixing region. It has been observed [see, e.g., Dimotakis (1986)] that, in spatially growing shear layers, an unequal amount of fluid is entrained from each of the freestreams, resulting in a mixed fluid that favors the high-speed fluid. The first experiments to show this were the incompressible, variable-density shear layer experiments of Brown and Roshko (1974). Brown (1974) showed that the fluid associated with the higher velocities had higher entrainment rates into the mixing layer. For these accelerated problems the large velocities are associated with the low density, consistent with the entrainment argument.

The mean presure gradient is obtained from eq. (9) and plotted, normalized by the hydrostatic pressure, in Fig. 2 for both cases. For the NCD case, the mean pressure is close to the hydrostatic balance. As time evolves, the mean pressure remains at this value. For the FVD case, the mean pressure gradient is initially lower than the hydrostatic balance. This plot shows that the mean pressure gradient for case FVD varies more in time. Again, as the density fluctuations decay, the mean pressure gradient approaches the hydrostatic balance.

Figure 3 plots the values of each term in the equation for the mean pressure gradient [eq. (9)] for case FVD. In this case, in the limit as the den-

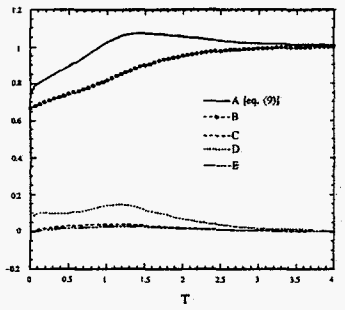

Figure 3. Evolution of terms in the mean pressure gradient [eq. (9)] for FVD case

sity variations tend to zero, the mean pressure gradient tends to the value $\overline{\rho}g = 1$. Initially, the mean pressure gradient is approximately 0.75 and the acceleration term, $g/\overline{v}$, is approximately 0.67. The correlation $\overline{v'(\partial p'/\partial x_3)}$ (labeled "D") is approximately 0.08 and represents 11 percent of the initial mean pressure gradient. All other terms are initially nearly zero. As the flow develops the mean pressure gradient increases to a value slightly larger than 1.0. At the last time shown it has very nearly a constant value of 1.0, which is consistant with the Boussinesq approximation. The second and third terms in the equation (9) for the mean pressure gradient grow slightly from their nonzero values and contribute only a few percent to the total mean pressure gradient. The correlation $\overline{v'(\partial p'/\partial x_3)}$ remains a large contribution to the mean pressure gradient up to late times.

Figure 4a shows $\overline{v'(\partial p'/\partial x_3)}/g\theta_0^2$ as a function of time for both cases. The magnitude of this correlation increases with initial density fluctuations. The nonzero value at the initial time represents a "rapid" part of this correlation. This correlation increases in time due to the "slow" part which is analogous to a drag for the mass flux. At late times this correlation is decaying and represents slow part decrease in the drag for the turbulent mass flux (see below in this section).

The correlation, $\overline{v'(\partial p'/\partial x_i)}/g\theta_o^2$, has been postulated by some modelers to behave as a "drag" term which impedes the growth of the turbulent mass flux [see, e.g., Besnard, et al., (1992)]. We have shown that the presence of this correlation impedes the growth of the turbulent mass flux. These results, however, suggest that this correlation behaves as both a "drag" or "slow" term and as a "rapid" term. The instant that the fluid is accelerated, this correlation immediately ("rapidly") takes a nonzero value, even though the mass flux is zero. To understand how this correlation behaves as a function of the mass flux, it is plotted as a function of the mass flux in

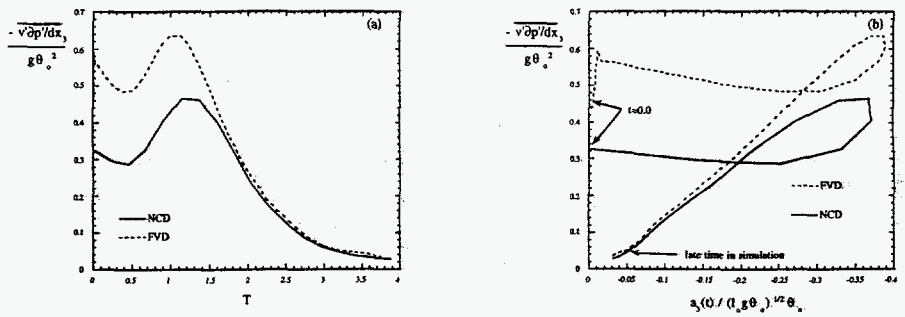

Figure 4. (a) $-\overline{v' \partial p'/\partial x_3}/g\theta_o^2$ vs. T and (b) $-\overline{v' \partial p'/\partial x_3}$ vs. a_3 for both cases

Fig. 4b. Initially, $-\overline{v'(\partial p'/\partial x_3)}$ is approximately 0.32 for case NCD and approximately 0.56 for case FVD. At $T = 0$, when the acceleration is applied, the dominant part of $\overline{v'(\partial p'/\partial x_3)}$ is the "rapid" part. As the flow evolves, the "rapid" part vanishes as the density fluctuations decay and the "drag" part increases causing an increase in $\overline{v'(\partial p'/\partial x_3)}$. Ultimately, at late times, the "drag" or "slow" part is dominant as the "rapid" part has vanished so that $\overline{v'(\partial p'/\partial x_3)}$ decays nearly linearly with the mass flux. At late times in this buoyancy-driven turbulent flow this correlation represents a "drag" on turbulent mass flux.

6. Model Comparisons

In this section we address the efficacy of the extensions of traditional k-ϵ model formulation and a heuristic two-point closure to variable-density turbulence.

6.1. MODEL OF BESNARD, HARLOW, RAUENSAHN AND ZEMACH

The model of Besnard, Harlow, Rauensahn and Zemach (herein refered to as the "one-point model") is an extension of one-point k-ϵ closures to variable-density turbulence. For the incompressible case, this model includes equations for R_{ij}, the turbulent energy dissipation rate, species concentrations, and correlations for the density-velocity and specific volume-density fluctuations. The higher-order unknowns in these equations are closed using typical constant density assumptions [e.g., Launder, Reece and Rodi (1975)] suitably extended to account for a variety of variable-density effects. The details of the model can be found in Besnard et al. (1992).

The model equations are derived for general inhomogeneous flows at

high Reynolds number. They are rewritten here for the specific case of a statistically homogeneous, variable-density fluid subjected to an acceleration. The evolution equation for the correlation between the specific volume and the density fluctuations, i.e., $b = -\overline{\rho' v'}$, [eq. (50) in Besnard et al. (1992)] reduces to

$$\frac{\partial b}{\partial t} = -c_{1b}\left(\frac{2\overline{\rho}\epsilon}{R_{nn}}\right) b. \tag{12}$$

A modified turbulent mass flux model equation is

$$\frac{\partial a_n}{\partial t} = (1 - c_{3a})\frac{b}{\overline{\rho}}\frac{\partial \overline{P}}{\partial x_n} - c_{1a}\left(\frac{2\overline{\rho}\epsilon}{R_{nn}}\right)\frac{a_n}{b^m} - c_{1aa}\frac{\sqrt{a_n a_n}}{K^{3/2}}\frac{a_n}{b^m}. \tag{13}$$

The details of the proposed modifications may be found in Sandoval (1995). Note that this model corresponds exactly to the development in BHRZ if $m_1 = 0$, $m_2 = 0$, $c_{3a} = 0$, $c_{1aa} = 0$. (For consistency with the definitions used in this study, the sign of a_i is the negative of that given by Besnard et al. (1992).) The kinetic energy equation is

$$\frac{\partial R_{nn}}{\partial t} = 2a_n\frac{\partial \overline{P}}{\partial x_n} - 2\overline{\rho}\epsilon. \tag{14}$$

Finally, the energy dissipation equation [eq. (51)] becomes

$$\frac{\partial \epsilon}{\partial t} = c_{3\epsilon}\left(\frac{2\overline{\rho}\epsilon}{R_{nn}}\right) a_n\frac{\partial \overline{P}}{\partial x_n} - c_{2\epsilon}\left(\frac{2\overline{\rho}\epsilon}{R_{nn}}\right)\epsilon. \tag{15}$$

The time scales for dissipation of a_n and b are "constructed" from a time scale associated with the energy cascade, $\tau \sim R_{nn}/(\rho\epsilon)$. This assumption is based on (1) turbulence characterized by a "large" inertial range where the dissipation rate is independent of viscosity (or diffusivity) and (2) that this cascade also dominates the dissipation of "a_n" and "b". This assumption is questionable for the case of initially quiescent, turbulence subjected to an acceleration. Thus the DNS provides a stern test of the single-point model.

6.2. MODEL OF CLARK AND SPITZ

The model of Clark and Spitz (herein referred to as the "two-point model") (1994) is a two-point (spectral) phenomenological model. The advantage of a two-point (spectral) formulation is that it eliminates the need for length-scale/dissipation equations and corollary assumptions which are employed in one-point modeling. The two-point model is an attempt to relieve some of the limitations inherent in the one-point k-ϵ or R_{ij}-ϵ formalism. Details of the development may be found in Clark and Spitz (1994).

The derivation of the model gives a hierarchical structure similar to that of the one-point model. The model equations (used in this study), are

$$\frac{\partial b(k,t)}{\partial t} = -\frac{\partial}{\partial k}\left\{\left(\frac{C_{bR1}}{\theta_R(k)} + \frac{C_{ba1}}{\theta_a(k)} - \frac{C_{bA1}}{\theta_A(k)}\right) k b(k,t)\right\}$$

$$+\frac{\partial}{\partial k}\left\{\left(\frac{C_{bR2}}{\theta_R(k)} + \frac{C_{ba2}}{\theta_a(k)} + \frac{C_{bA2}}{\theta_A(k)}\right) k^2 \frac{\partial b(k,t)}{\partial k}\right\} - 2\overline{D}k^2 b(k,t), \qquad (16)$$

$$\frac{\partial a_n(k,t)}{\partial t} = -\frac{\partial}{\partial k}\left\{\left(\frac{C_{aR1}}{\theta_R(k)} + \frac{C_{aa1}}{\theta_a(k)} - \frac{C_{aA1}}{\theta_A(k)}\right) k a_n(k,t)\right\}$$

$$+\frac{\partial}{\partial k}\left\{\left(\frac{C_{aR2}}{\theta_R(k)} + \frac{C_{aa2}}{\theta_a(k)} + \frac{C_{aA2}}{\theta_A(k)}\right) k^2 \frac{\partial a_n(k,t)}{\partial k}\right\}$$

$$-\left\{\frac{C_{RP1}\beta_{RP1}}{\theta_a(k)} + \frac{C_{RP2}\beta_{RP2}}{\theta_R(k)}\right\} a_n(k,t)$$

$$-\left[1 - C_{vdp}\right]\frac{b(k,t)}{\overline{\rho}}\frac{\partial \overline{P}}{\partial x_n} - \left[\frac{\overline{\mu}}{\overline{\rho}} + \overline{D}\right] k^2 a_n(k,t), \qquad (17)$$

and

$$\frac{\partial R_{nn}(k,t)}{\partial t} = -\frac{\partial}{\partial k}\left\{\left(\frac{C_{R1}}{\theta_R(k)}\right) k R_{nn}(k,t)\right\} + \frac{\partial}{\partial k}\left\{\left(\frac{C_{R2}}{\theta_R(k)}\right) k^2 \frac{\partial R_{nn}(k,t)}{\partial k}\right\}$$

$$-2a_n(k,t)\frac{\partial \overline{P}}{\partial x_n} - 2\frac{\overline{\mu}}{\overline{\rho}}k^2 R_{nn}(k,t) \qquad (18)$$

where

$$\theta_R(k) = \left[\frac{1}{\overline{\rho}}\int_0^k q^2 R_{nn}(q)dq\right]^{-1/2}, \quad \theta_a(k) = \left[k^2\sqrt{a_n(k,t)a_n(k,t)}\right]^{-1},$$

$$\theta_A(k) = \left[k\sqrt{a_n(t)a_n(t)}\right]^{-1},$$

where β_{RP1} and β_{RP2} are chosen to be $1/b(t)$, and

$$b(t) = -\int_0^\infty b(k,t)dk, \;\; a_i(t) = \int_0^\infty a_i(k,t)dk, \;\; R_{ij}(t) = \int_0^\infty R_{ij}(k,t)dk.$$

The original formulation by Clark and Spitz did not include C_{vdp}.

6.3. RESULTS

Comparisons are made between the DNS data (for case FVD), and the modified one-point and two-point models. For this investigation the following one-point model coefficients are used: $c_{1b} = 1.0$, $c_{2\epsilon} = 1.92$, $c_{3\epsilon} = 1.61$, $c_{3a} = 0.0$, $c_{1a} = 2.2$, $m_2 = 1.0$, $c_{1a} = 0.0$, and $c_{1aa} = 1.5$. The initial values are: $R_{nn}(t=0) = 3.006(10)^{-4}$, $b(t=0) = 0.5$, $a(t=0) = 0.0$ and $\epsilon(t=0) = 8.7979(10)^{-7}$. A parameter study showed that caluations with this one-point model showed extreme sensitivity to the choice of $\epsilon(t=0)$. The value for $\epsilon(t=0)$ is chosen in order to give the correct length scale of b which in turn gives the correct early time trajectory of a_n. For this investigation the following two-point model coefficients are used: $C_{RP1} = 0.125$, $C_{vdp} = 0.35$, $C_{aa1} = C_{aA1} = -.2424$, $C_{R1} = C_{aR1} = C_{bR1} = \sqrt{6}C_k^{-3/2}/11$, $C_{R2} = C_{aR2} = C_{bR2} = 2\sqrt{6}C_k^{-3/2}/11$; all other coefficients being set to zero. C_k is the Kolmogorov constant, chosen to be 3/2. The initial spectra for $b(k)$ and $R_{nn}(k)$ taken from the DNS are used for initial conditions in the two-point model; in addition $\overline{\rho} = 1$ and $\overline{\mu} = \overline{D} = 8.543(10)^{-3}$. The comparison between the two-point model and the DNS is made by examining one-point statistics.

Figure 5a shows the evolution of b for the DNS and the model results. The modified one-point model for the decay of b is somewhat different then the DNS result. The initial value for ϵ is artificially small, leading to an inadequate dissipation of b at the early times. This may represent a deficiency in the methodology of one-point closures and also suggest an inclusion of molecular diffusive and viscous effects in the one-point formulation. The flows studied in the DNS simulations are dominated by viscous diffusion, at early and late times and this is not accounted for in the one-point model. Thus, we can choose ϵ to give either the correct energy dissipation, or the correct turbulent time-scale, or the correct length scale of b, but not all three. Therefore, b does not dissipate fast enough and, as a result, the subsequent behavior of b is incorrect although the initial growth rates of a and R_{nn} are adequate (see Figure 5b and 5c). At late stages, the values of a and R_{nn} are overpredicted, probably due to an overprediction of b.

The two-point model which does include molecular viscous and diffusive effects does substantially better at predicting the evolution of b. As a consequence, it does better at late times for both a and R_{nn} than the one-point model. This model does slightly overpredict the values of a and underpredicts the value of R_{nn} at their extrema; the one-point model does slightly better here.

Figure 5d shows the evolution of $\partial\overline{p}/\partial x_n$ for the DNS and the models.

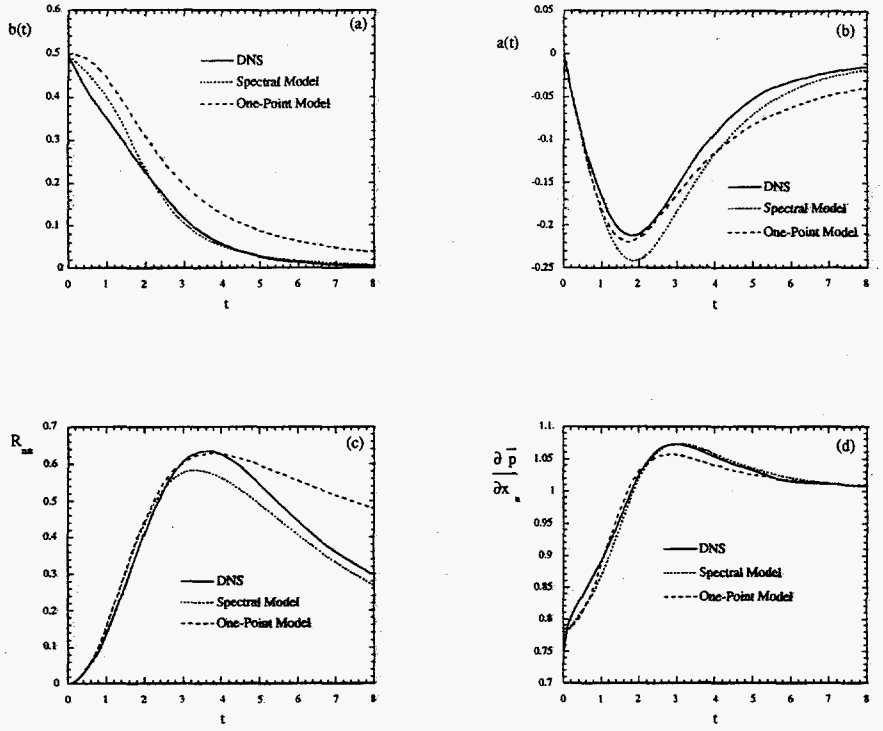

Figure 5. Evolution of (a) b, (b) a, (c) R_{nn} and (d) $\partial\overline{P}/\partial x_3$ for DNS case FVD and the one-point and two-point models

The model comparisons show relatively good agreement with the DNS.

7. Conclusions

Direct numerical simulations of homogeneous variable-density turbulence subjected to an acceleration have been performed using a pseudo-spectral algorithm. The range of density fluctuations exceeds the limits of validity of the so-called Boussinesq approximation. The overall statistical behavior of the flow resembled, to some degree, that of the Boussinesq-limited calculations of Batchelor et al., and is characterized by three phases; (1) Initially growing turbulence when the acceleration acts on the density variations, (2) a period of time when the energy and turbulence mass flux reach their extrema, and (3) a period of decay when the energy, and turbulent mass flux decrease. Because there is no source of density fluctuations in these homogeneous simulations, the density fluctuations decrease monotonically

in time.

The results of the direct numerical simulations indicate that the correlation $\overline{v'\partial p'/\partial x_i}$ can be considered the sum of a "slow part" and a "fast part", in analogy with the well-known decomposition of pressure-strain correlations of constant density turbulence. This modification, among others was incorporated into a single-point model and a two-point model of variable density turbulence. Predictions of the modified models are compared to the DNS results, and indicate that two-point model performed slightly better than the one-point model. It is suggested that the one-point model should be extended further to account for molecular effects at early times and to permit a length scale for the density fluctuations that is independent of the length scales for the velocity fluctuations.

References

Andronov, A., Bakhrakh, S. M., Meshkov, E. E., Mokhov, V. N., Nikiforov, V. V., Pevnitskii, A. V., and Tolshmyakhov, A. I., 1982, Sov. Phys. Dolk., **27**, 393

Batchelor, G. K., Canuto, V. M. and Chasnov, J. R., 1992, "Homogeneous buoyancy-driven turbulence", J. Fluid Mech, **235**

Besnard, D., Harlow, F. H., Rauenzahn, R. M., and Zemach, A. C., 1992, Turbulence Transport Equations for Variable-Density Turbulence and Their Relationship to Two-Field Models, Report No. LA-12303-MS, Los Alamos National Laboratory

Bird, R. B., Stewart, W. E. and Lightfoot, E. N., 1960, Transport Phenomena, John Wiley & Sons

Brown, G. L. and Roshko, A., 1974, "On density effects and large structure in turbulent mixing layer", J. Fluid Mech, **64**

Brown, G. L., 1974, "The Entrainment and Large Structue in Turbulent Mixing Layers", Fifth Australasian Conference on Hydraulics and Fluid Mechanics, at University of Canterbury, New Zealand

Clark, T. T., and Spitz, P., 1994, A Spectral Model for Variable-Density Turbulence, Report No. LA-12671-MS , Los Alamos National Laboratory

Cranfill, C., 1992, "A New Multifluid Turbulent-Mix Model", Report No. LA–UR-92-2484, Los Alamos National Laboratory

Dimotakis, P. E., 1986, " Two-Dimensional Shear-Layer Entrainment", AIAA Journal, **24**,11

Eswaran, V. and Pope, S. B., 1988, "Direct numerical simulations of turbulent mixing of a passive scalar", Phys. Fluids, **31**, 3

Joseph, D. D., 1990, "Fluid Dynamics of two miscible liquids with diffusion and gradient stresses", Eur. J. Mech., B/Fluids, **9**, 6,

Launder, B. E., Reece, G. J. and Rodi W, 1975, "Progress in the development of a Reynolds- stress turbulence closure", J. Fluid Mechanics, **68**

Leith, C. E., 1967, "Diffusion Approximation to Internal Energy Transfer in Isotropic Turbulence", Phys. Fluids, **10** (7)

McMurtry, P. A., 1987, PH.D thesis, University of Washington

Sandoval, D. L., 1995, "The dynamics of variable-density turbulence" Dissertation, University of Washington, (also Report No. LA-13037-T, Los Alamos National Laboratory, 1995).

Zeman, O. and Lumley, J. L., 1976, "Modeling Buoyancy Drive Mixed Layers" J. of Atmos. Sciences, **33**